

Mesoscale Snow Bands in an Ocean-Effect Snowstorm

Frank P. Colby, Jr. *
University of Massachusetts Lowell, Lowell, MA 01854

1. INTRODUCTION

Using the Penn State/NCAR Mesoscale Model version 5 (MM5) to simulate the atmosphere, the mesoscale structure of precipitation during the January 13-15, 1999, ocean-effect snowstorm in New England is investigated. During this storm, more than 25 cm of snow fell along the New England coastline. Mesoscale bands were observed during this storm, and this mesoscale structure is the focus of this modeling study. In this overview, results from an MM5 simulation are shown to illustrate the banded structures present in the model run.

2. MODEL CONFIGURATION

The MM5 was run for 48 hours of simulated time using 00 UTC Eta Model, 90km gridded output for boundary and initial conditions. The model was set up with 3 grids, as shown in Fig. 1. The outer grid had a 36 km grid size, and two-way interaction was used for the nested 12 km and 4 km grids. Simple ice physics (Dudhia, 1989) was employed and the MRF boundary layer parameterization (Hong and Pan, 1996) used. The Grell convective scheme (Grell, 1993) was applied in the 12 and 36 km grids, but no convective parameterization was used in the 4 km grid. The model was run with 34 sigma levels in the vertical, 13 of which were below 1.5 km to allow detailed representation of the boundary layer.

The model output was produced at one hour intervals, and processed into GrADS format (Grid Analysis and Display System – see <http://grads.iges.org/grads> for more details) using a Unix script.

3. SYNOPTIC-SCALE SETTING

The snow began along the coast around 18 UTC, January 13, 1999, and continued through 00 UTC, January 15, with occasional surges and lulls in intensity. Snow also fell inland, although in decreasing amounts as the distance from the coast increased.

At 18 UTC on the 13th, the leading edge of very cold, arctic air was just reaching the eastern coastline of southern New England. Figure 2 shows the temperature and pressure pattern at this time from the NWS reanalysis gridded dataset, while Fig. 3 shows

the corresponding horizontal wind field and vertical motion (omega) at 700 hPa. Notice the area of high pressure to the northwest, the downward vertical motion, and the northwest flow almost reaching the ocean in New England. By 06 UTC on the 14th of January, the flow was due north over New England, and the cold air had settled further to the south (Figs. 4 and 5).

By 15 UTC on the 14th, a shear zone began to develop along the coast, with strong northeast winds off-shore, and weak north winds inland. This shear zone continued to sharpen through 00 UTC on the 15th of January, as seen in Fig. 6. The temperature and pressure fields at this time are shown in Fig. 7.

4. MESOSCALE BANDED STRUCTURES

The occurrence of banded structures took place in different locations at different times during the 2-day period. There were two mesoscale bands that lasted longer than six hours, and three other bands with less well-defined structure. Below, three of these bands are illustrated with model output.

4.1 Southeast New Hampshire

What looked like one long-lived band formed along the New Hampshire coastline around 20 UTC on the 13th. Temperatures and winds are shown in Fig. 8 from the 4 km grid at this time, and it is clear that the low-level flow is confluent along the New Hampshire coastline. The vertical motion field appears in Fig. 9, showing the weak upward and downward couplet. By 00 UTC, January 14, the vertical motion pattern had become much more distinct (Fig. 10), and this lasted until about 06 UTC on the 14th, before dissipating. Figure 11 shows the vertical motion associated with the band at 03 UTC at a lower level, and Fig. 12 shows the same field at 06 UTC, when it had almost dissipated. This band moved inland with time, and the confluence associated with it moved inland as well, as can be seen in Fig. 13.

Figure 14 shows a cross-section drawn through the band at 03 UTC on the 14th, showing the vertical motion field superimposed on the temperature field, and including the horizontal wind barbs. The location of the cross-section is shown in Fig. 13. From this figure, it is clear that there are two bands, one below the temperature inversion at 900 hPa, and the other above. Both appear to move inland, but the lower band is the one associated with the confluent flow shown on Figs. 8 and 13. Figure 15 shows the same cross-section at 06 UTC, when the upper band is almost gone, and the lower band has weakened.

* Corresponding author address: Frank P. Colby, Jr., Dept. of Env., Earth, & Atmos. Sci., University of Massachusetts Lowell, Lowell, MA 01854; email: Frank_Colby@uml.edu

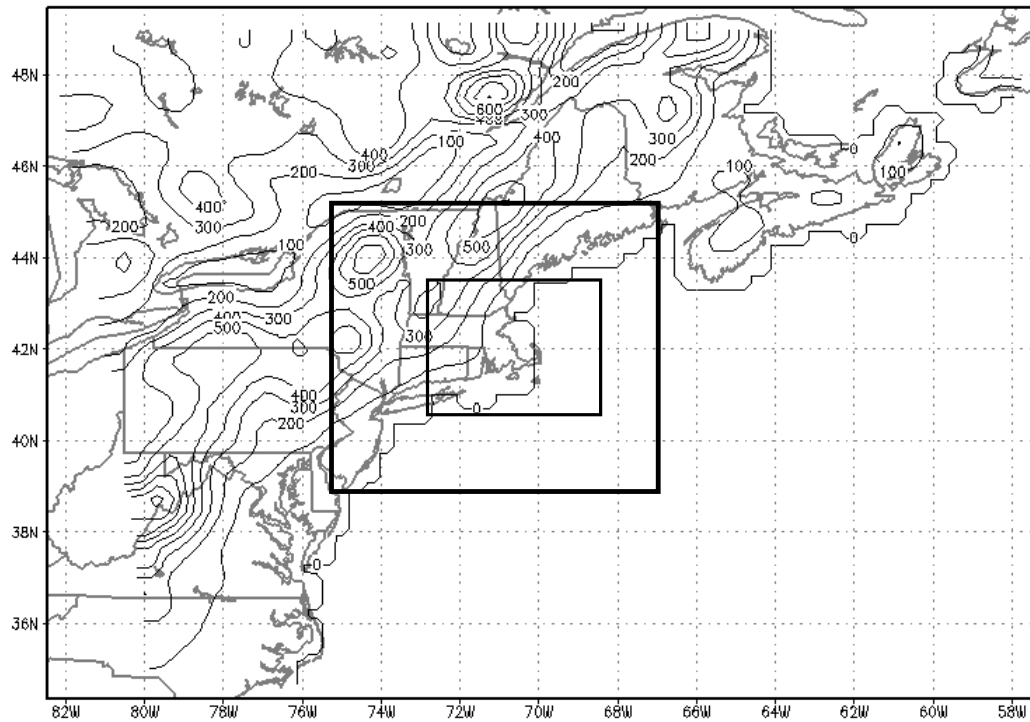


Figure 1. Map showing extent and location of the three different grids mentioned in the text. The outermost grid has a 36 km grid spacing, the intermediate grid has 12 km spacing, and the innermost grid has 4 km spacing.

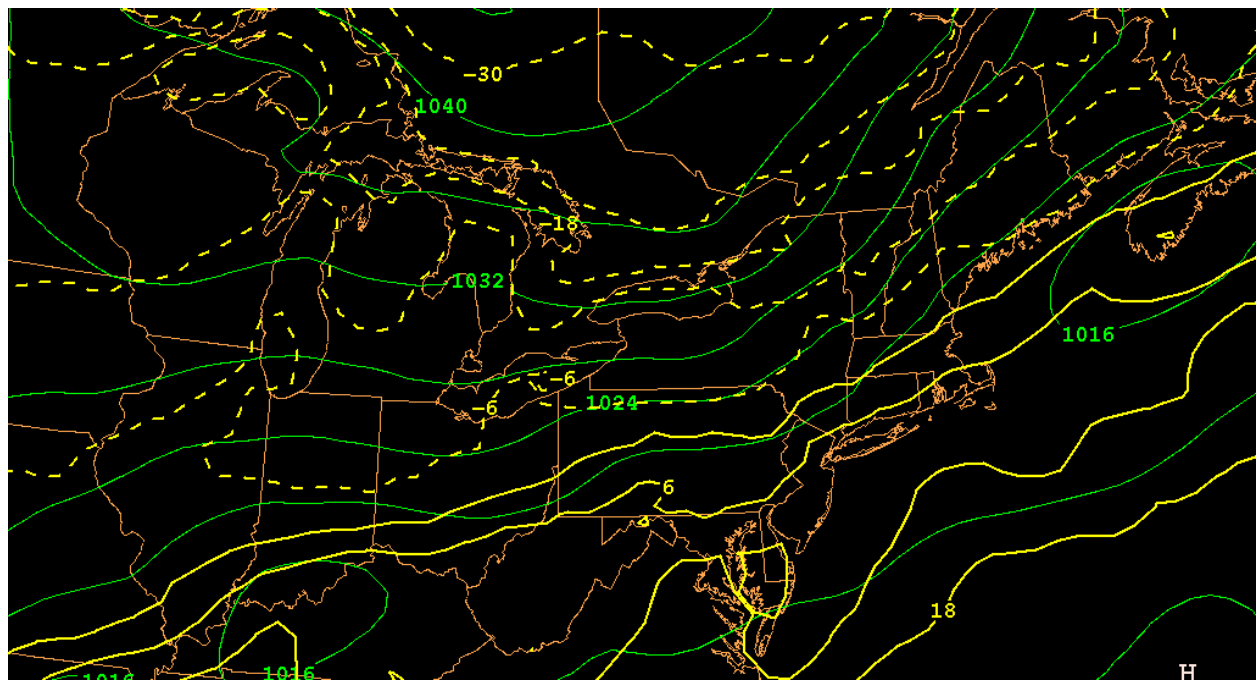


Figure 2. 1000 hPa Temperature ($^{\circ}\text{C}$) and sea-level pressure (hPa) from NWS reanalysis for January 13, 1999, 18 UTC.

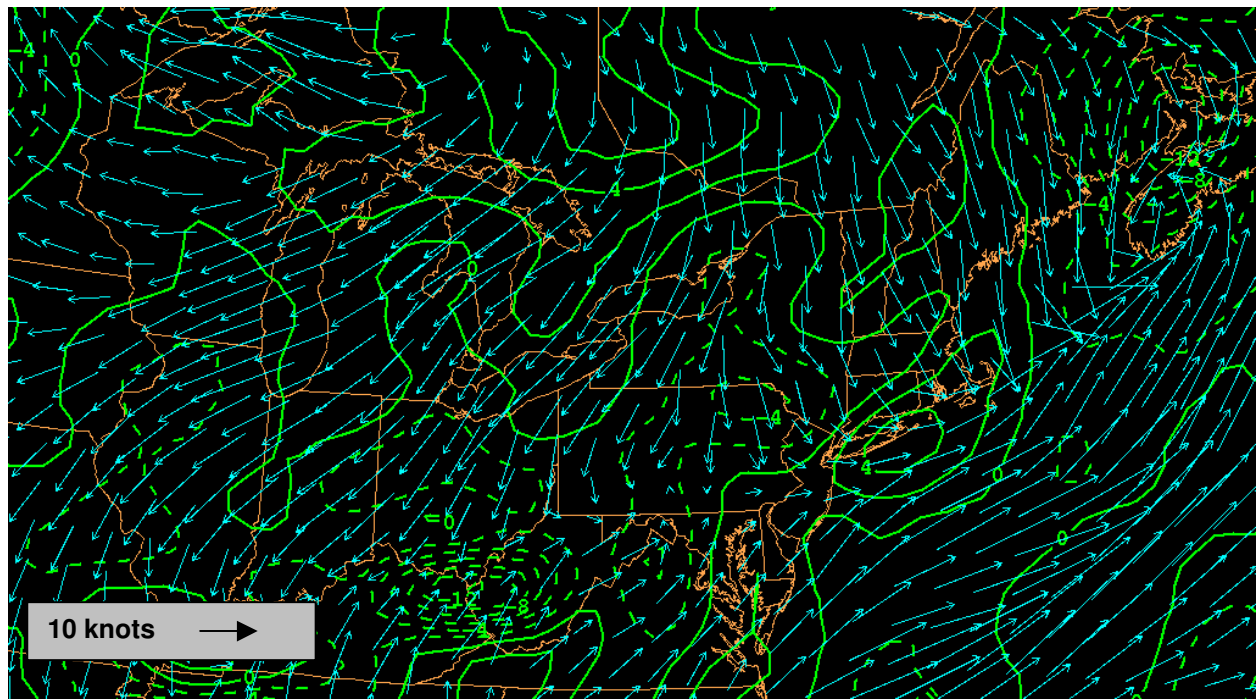


Figure 3. As in Fig. 2, except showing 1000 hPa horizontal wind field with arrows and 700 hPa omega (10^{-3} hPa/s). The scale for the conversion between length of arrow and wind speed is shown in the lower left corner.

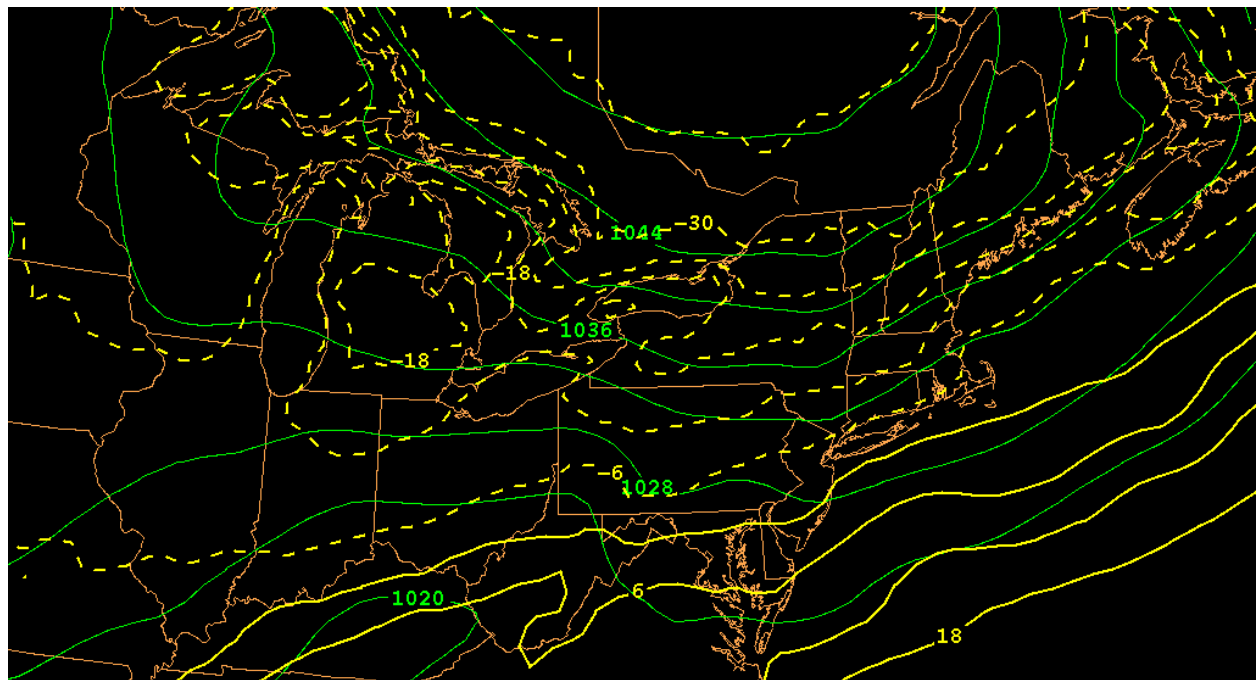


Figure 4. As in Fig. 2, except for 06 UTC, January 14, 1999.

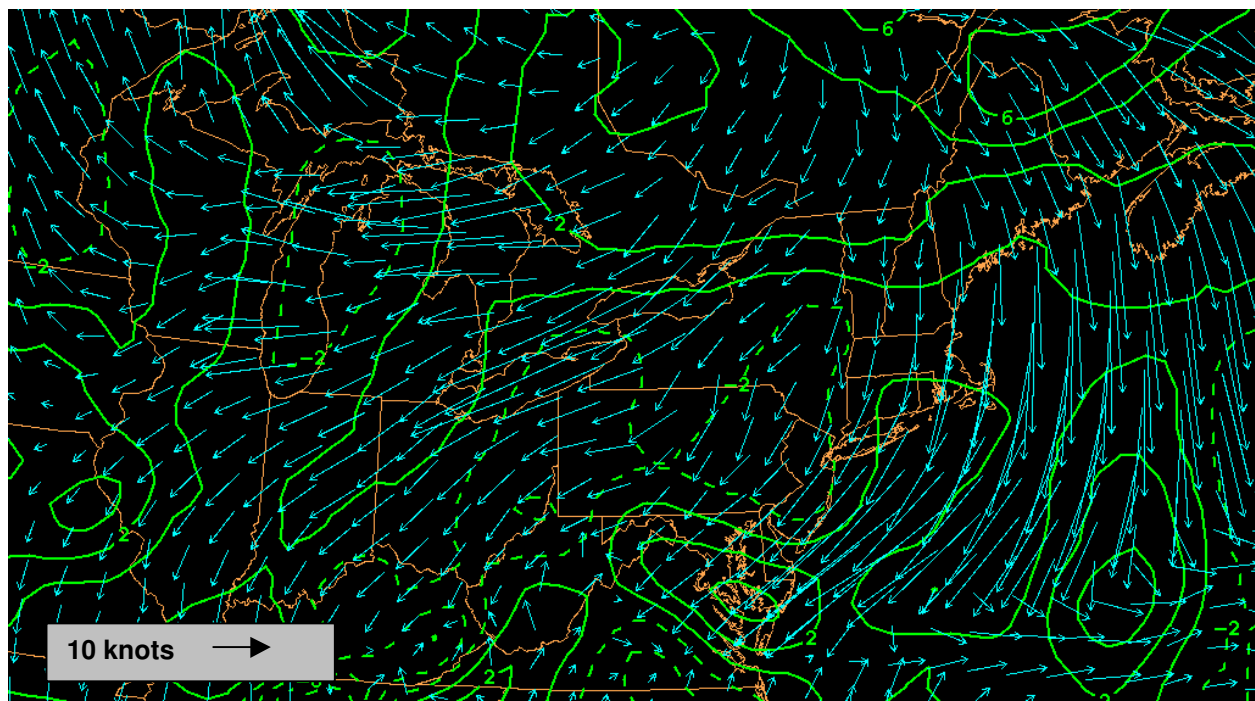


Figure 5. As in Fig. 3, except for 06 UTC, January 14, 1999.

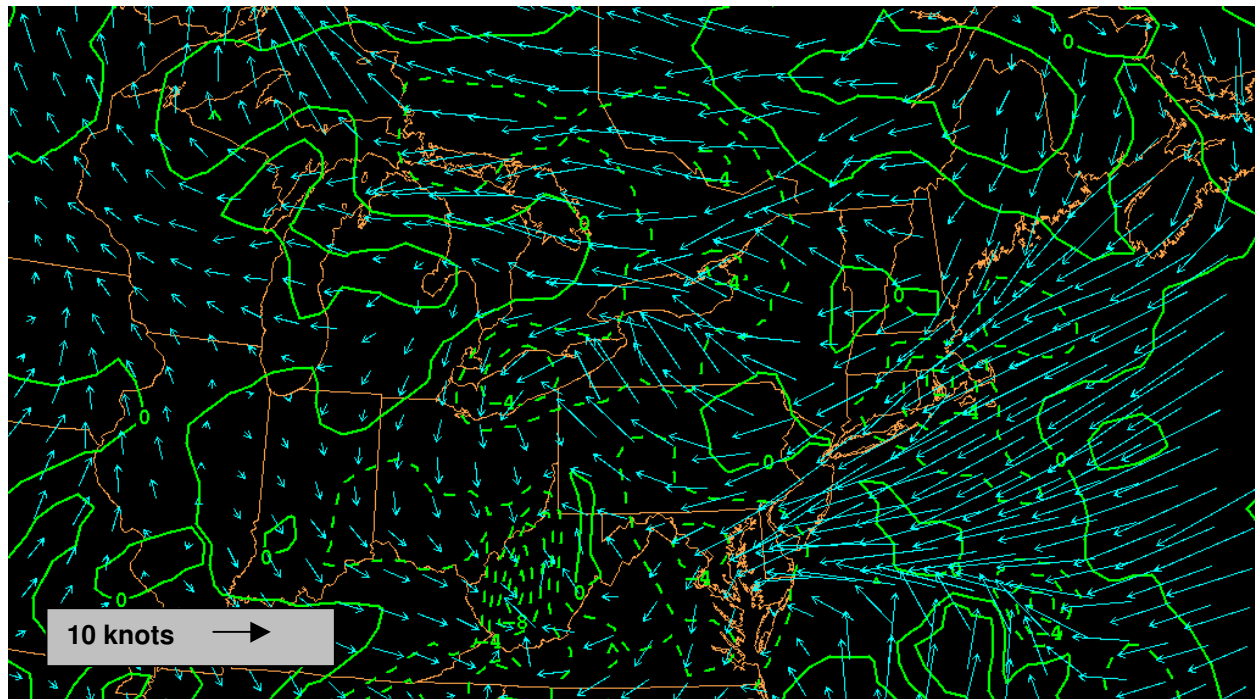


Figure 6. As in Fig. 5, except for 00 UTC, January 15, 1999.

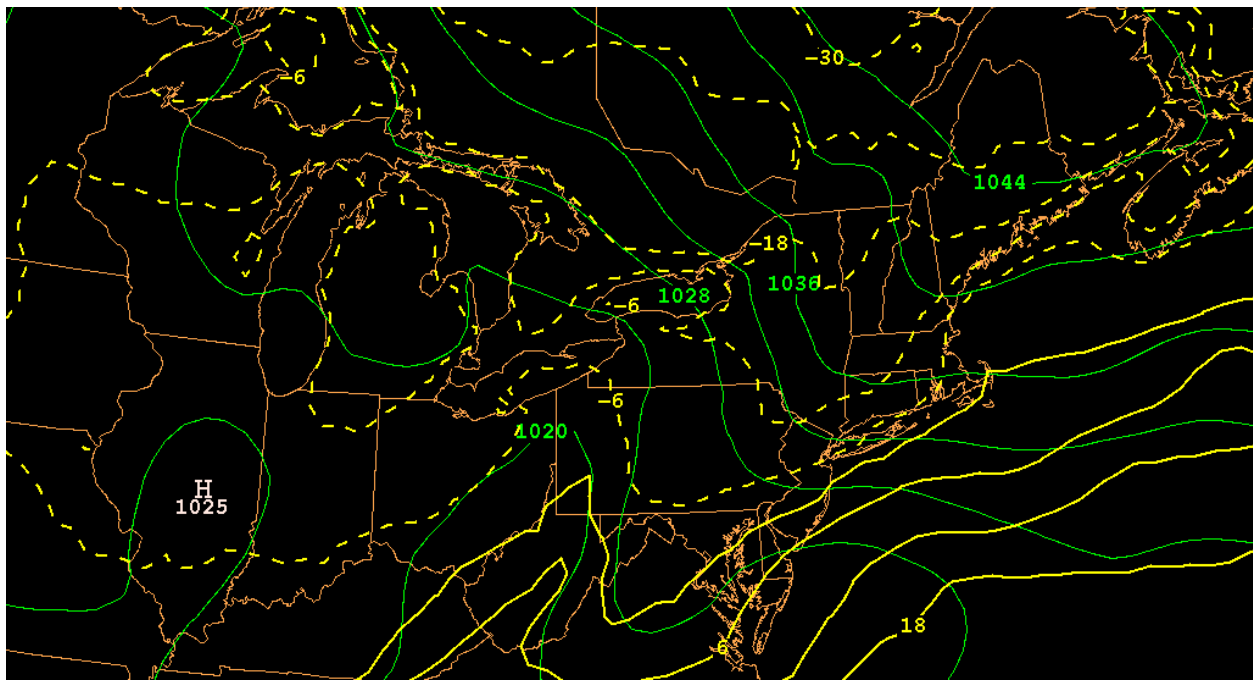


Figure 7. As in Fig. 4, except for 00 UTC, January 15, 1999.

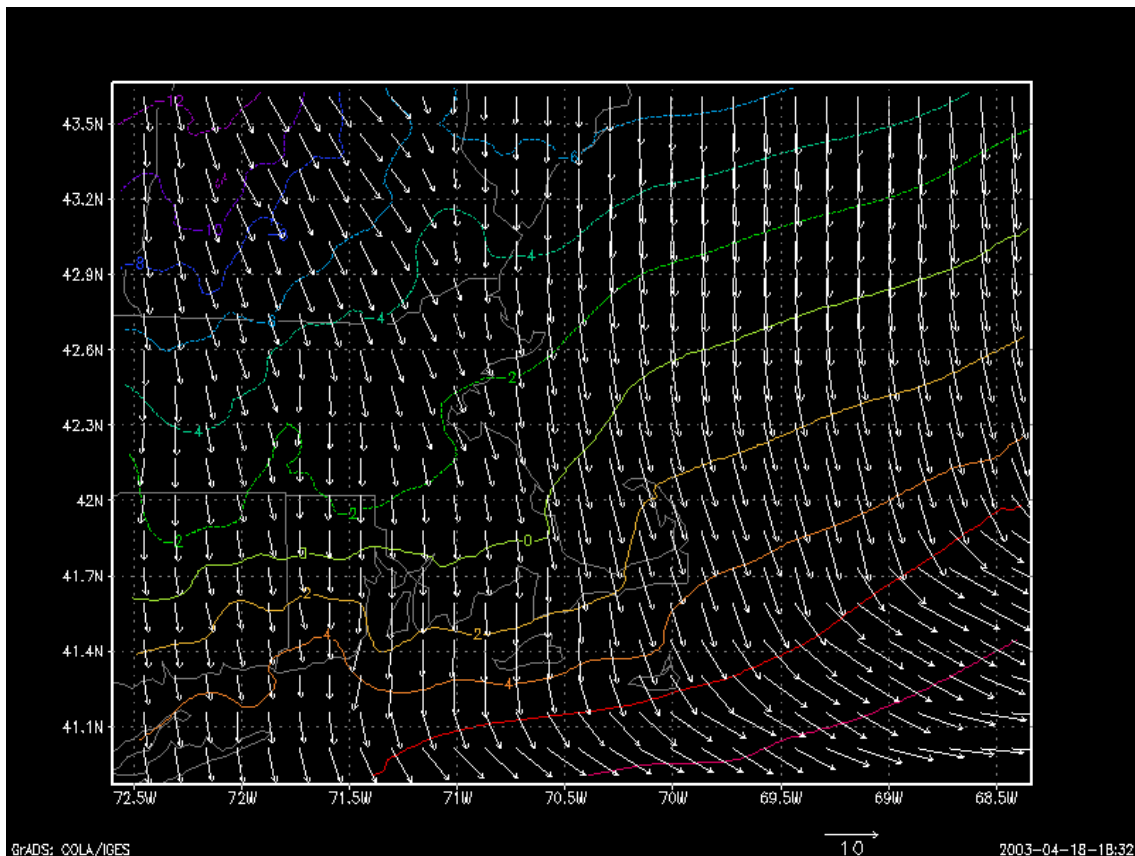


Figure 8. Winds (m/s) and temperatures ($^{\circ}\text{C}$) from the 4 km grid of the MM5 simulation, valid at 20 UTC, January 13, 1999. Scale for wind speed is in the lower right, and temperatures are contoured at 2°C intervals. Data is from the lowest model layer, about 25 meters above ground level.

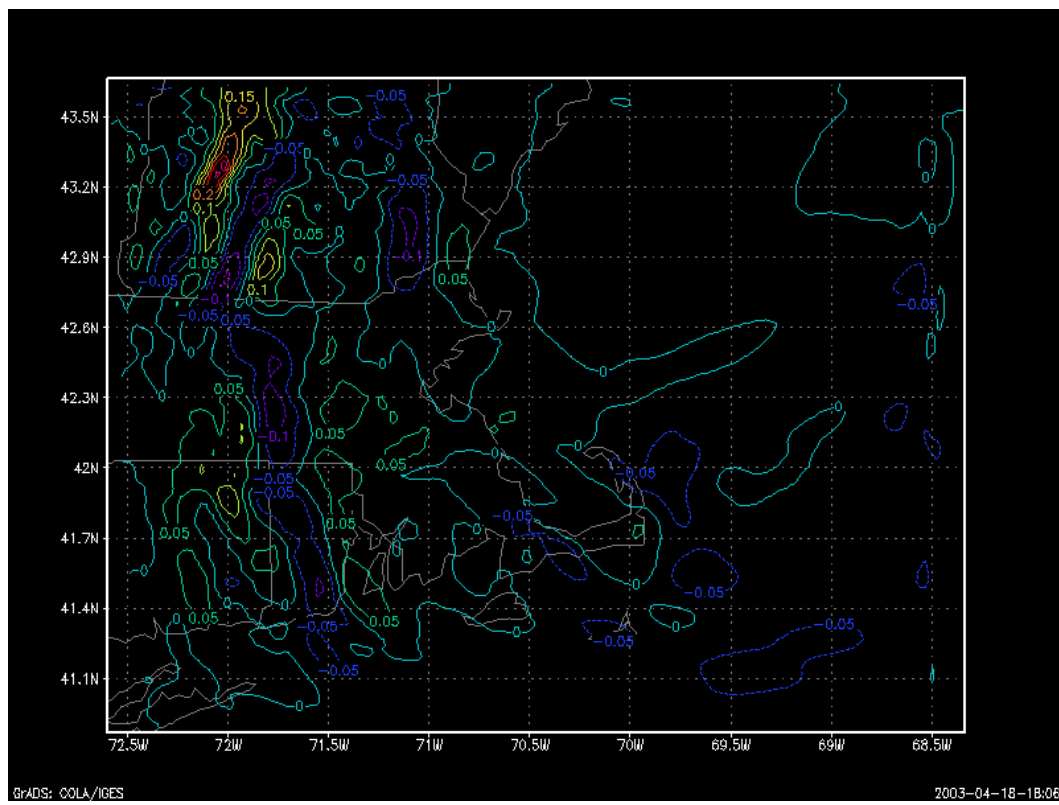


Figure 9. As in Fig. 8, except showing vertical motion (cm/s) at about 700 hPa.

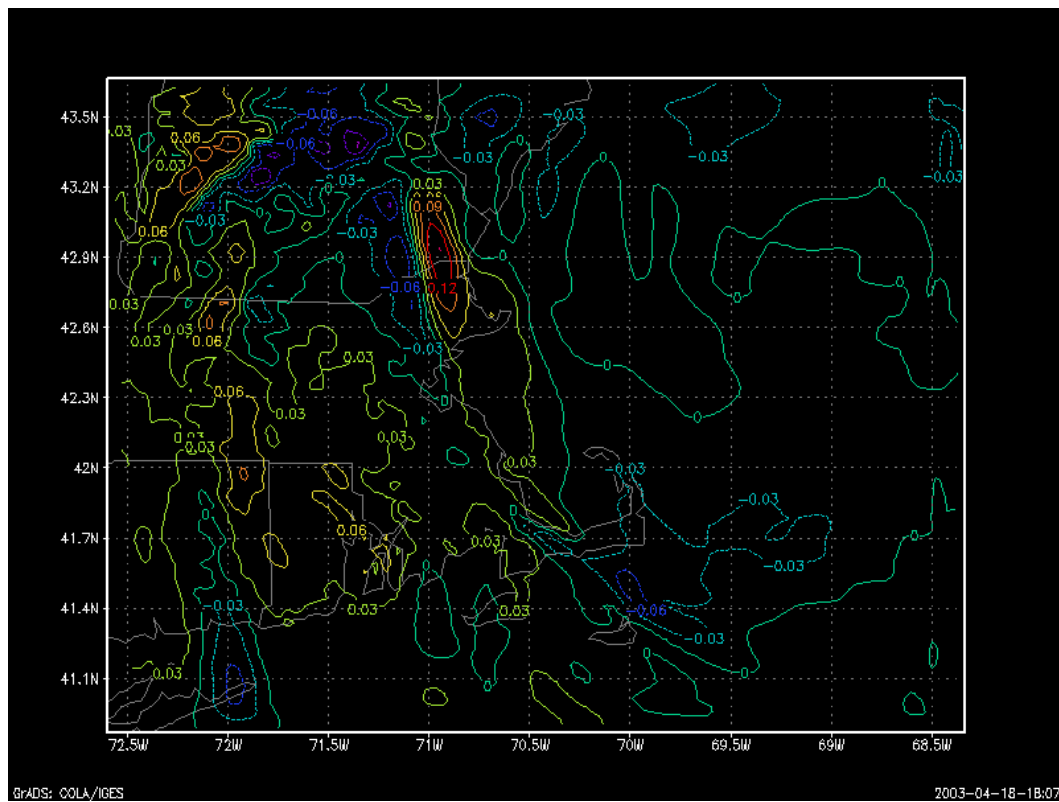


Figure 10. As in Fig. 9, except for 00 UTC, January 14, 1999.

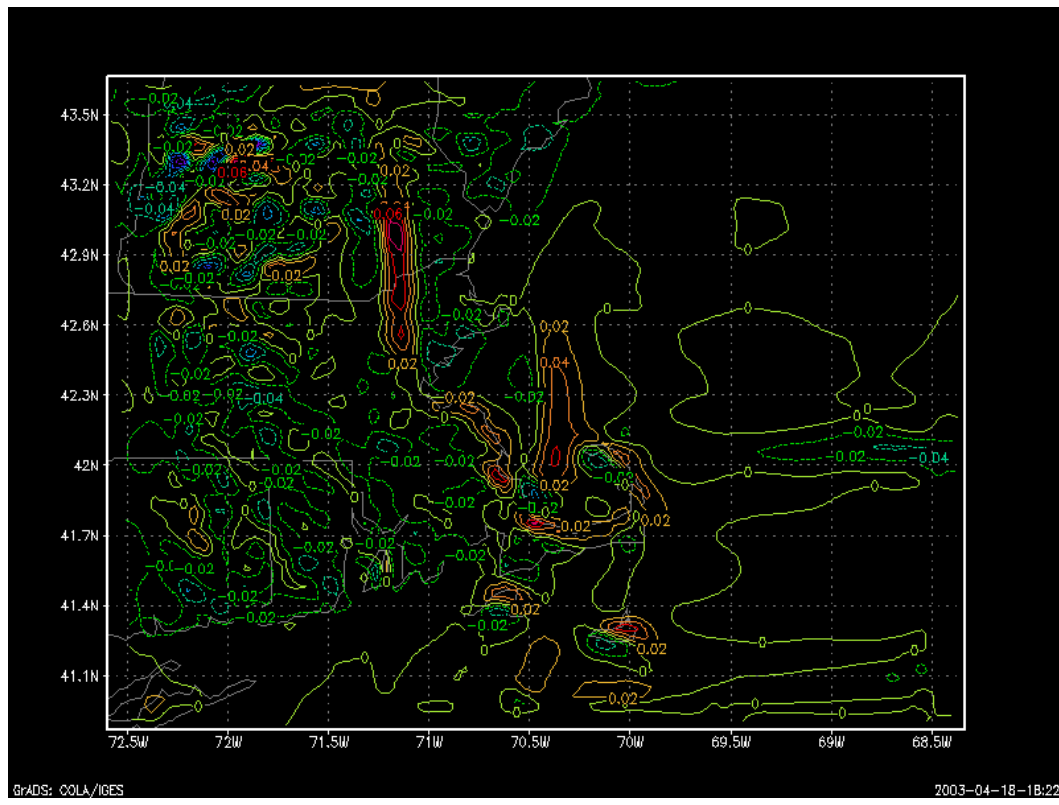


Figure 11. As in Fig. 10, except for 03 UTC at about 900 hPa.

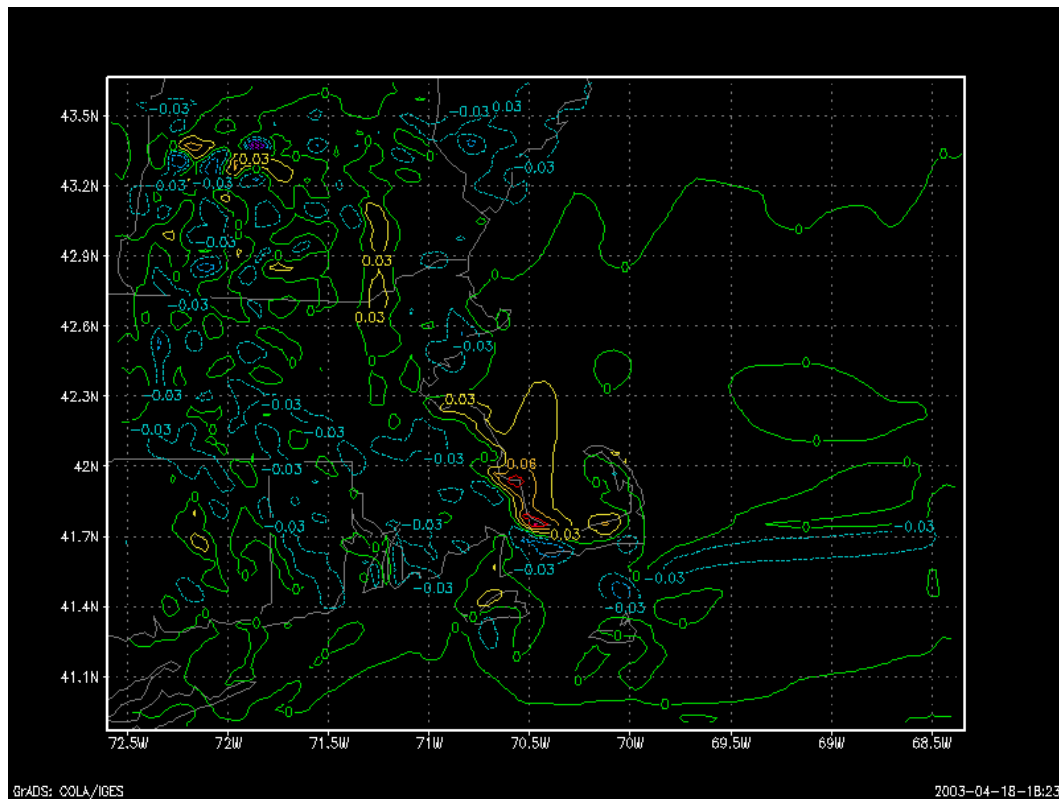


Figure 12. As in Fig. 11, except for 06 UTC.

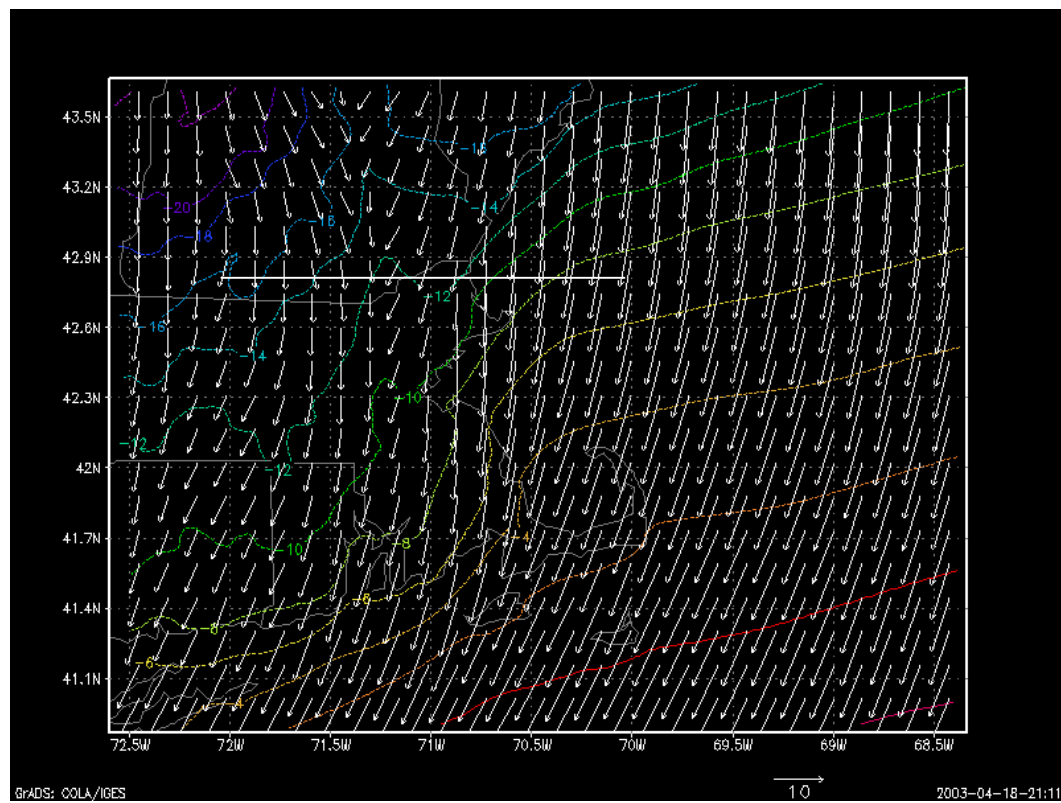


Figure 13. As in Fig. 8, except for 06 UTC, January 14, 1999. White line is the location of the cross-sections following.

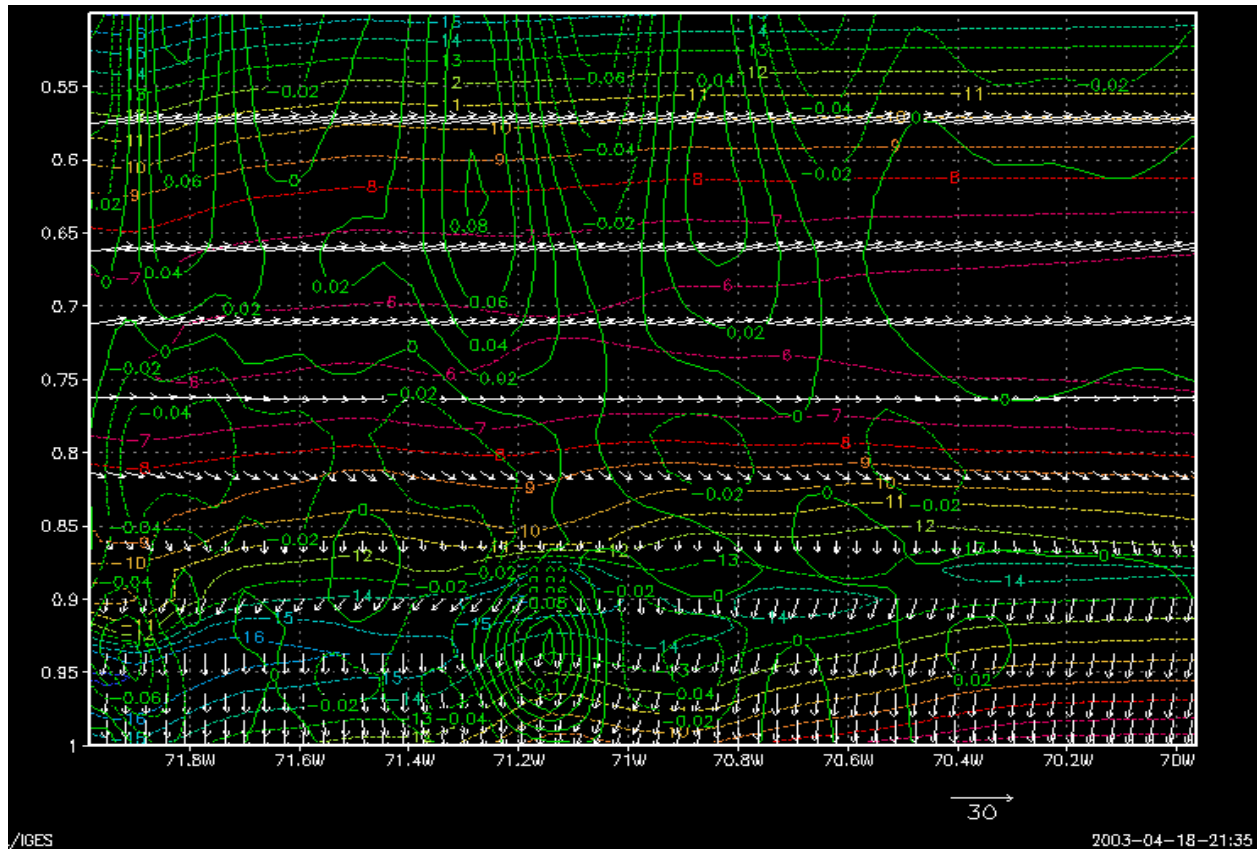


Figure 14. Vertical cross-section taken along the line shown in Fig. 13. Dotted lines are temperatures ($^{\circ}\text{C}$) contoured at 1 $^{\circ}\text{C}$ intervals. All of the temperatures are negative in this figure. Vertical motion (cm/s) is contoured in green. Horizontal winds are shown as arrows, scaled as in the lower right. Vertical scale is sigma (=pressure/surface-pressure).

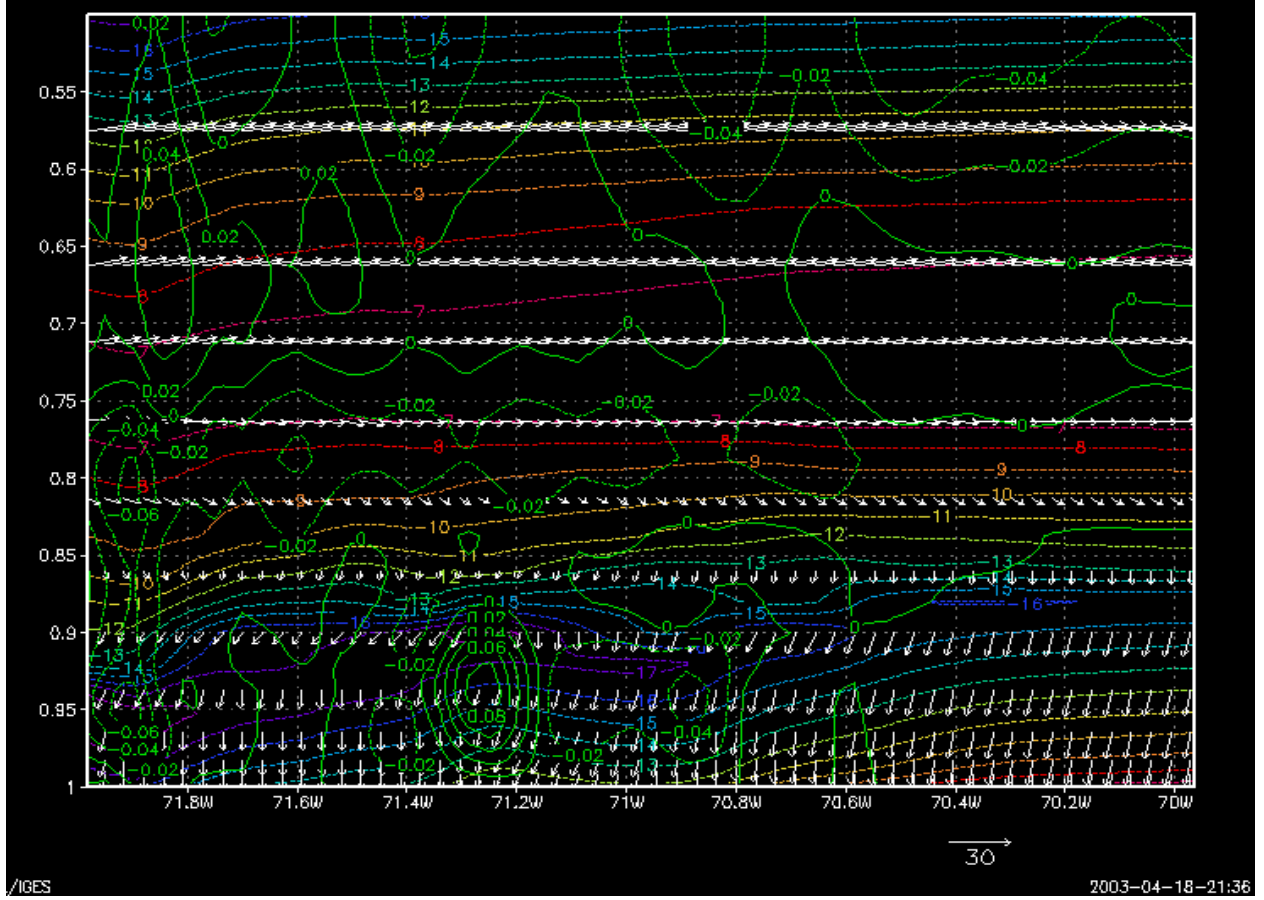


Figure 15. As in Fig. 14, except for 06 UTC.

4.2 Rhode Island Band

By 20 UTC on the 14th, a band was discernible in Rhode Island. This band, unlike the previous one, is mostly identifiable by the downward motion rather than the upward motion. The downward motion pattern shows up clearly in Figure 9, as part of a line of downward motion that runs from Rhode Island north-northwestward through Massachusetts and into New Hampshire. In Fig. 16, it is clear that the section in Rhode Island is separate from whatever was present at 20 UTC to the north. This band weakens as it moves off to the southwest, and by 00 UTC (Fig. 10), the band is moving out of the model domain. A cross-section through this band appears in Fig. 17 (see Fig. 16 for location of cross-section). Notice that the downward motion characterizing this band is found in the upper part of the figure, above the warmer temperatures near the surface.

4.3 Coastal Band

By 04 UTC on the 14th, low-level upward motion was found along the eastern coastline of New Hampshire and Massachusetts. After 21 UTC, the southern end

of this line became weaker, while the northern section strengthened. This band of upward motion appears to be frontal in character, with a strong horizontal temperature gradient, and low-level confluence in the horizontal winds.

Figure 18 shows the vertical motion at 12 UTC on the 14th, when this coastal front is clearly visible, and Fig. 19 shows the vertical motion at 18 UTC. The accompanying winds and temperatures appear in Fig. 20. By 00 UTC on the 15th, the line of vertical motion has extended into the interior of southeastern Massachusetts (see Figs. 21 and 22).

5. Conclusions

This paper illustrates three of the mesoscale bands that formed between 00 UTC, January 13 and 00 UTC, January 15, 1999. Some of these bands produced significant snowfall, with up to 25 cm accumulating along the eastern coastline of Massachusetts.

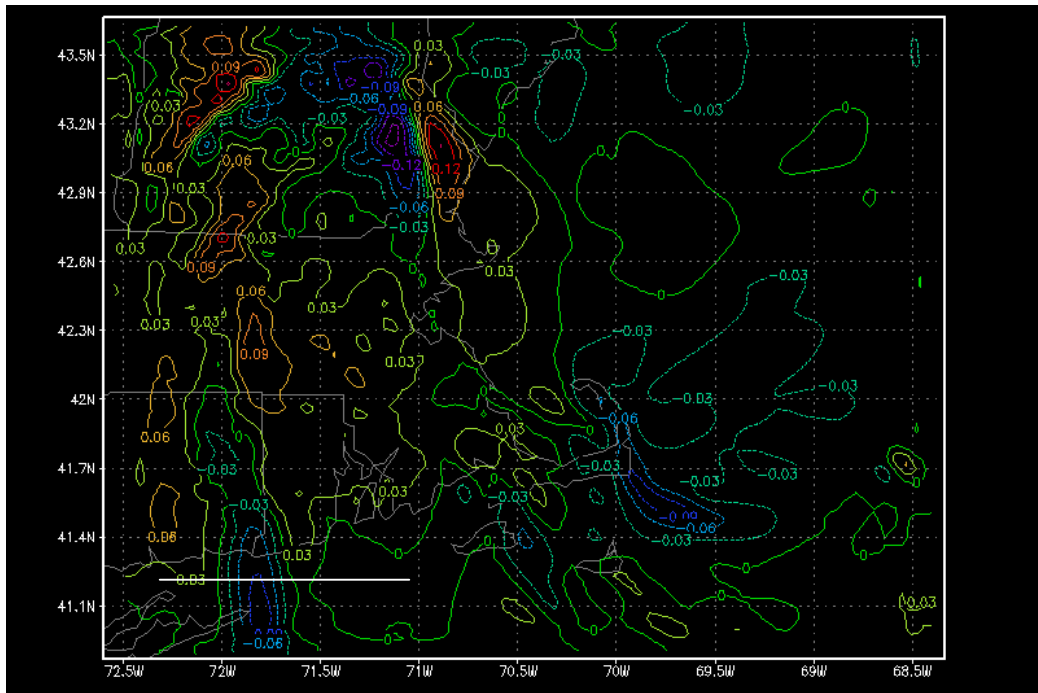


Figure 16. As in Fig. 9, except for 23 UTC, January 13, 1999. White line shows location of cross-section in Fig. 17.

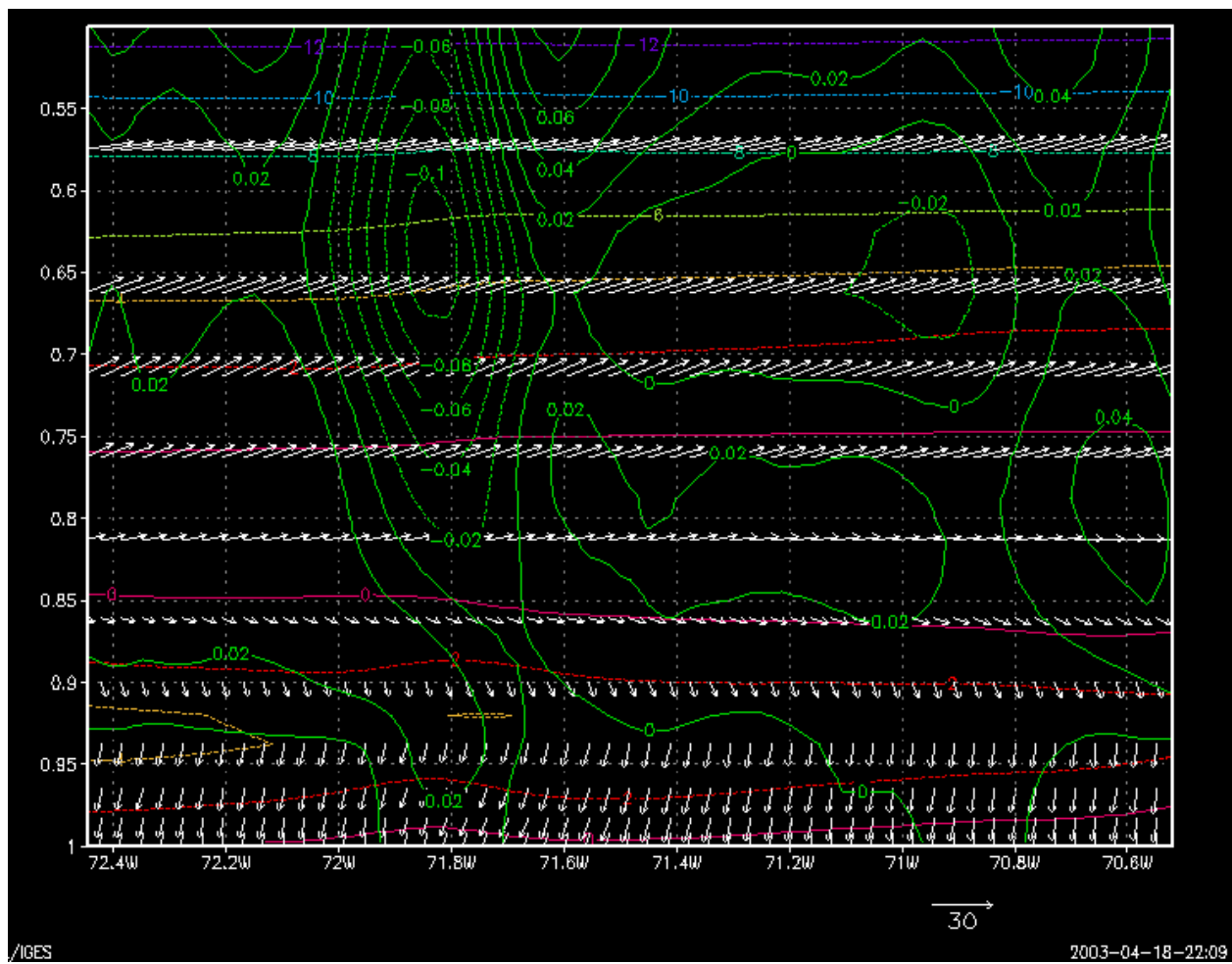


Figure 17. As in Fig. 15, except for location shown in Fig. 16, and for 23 UTC, January 13, 1999.

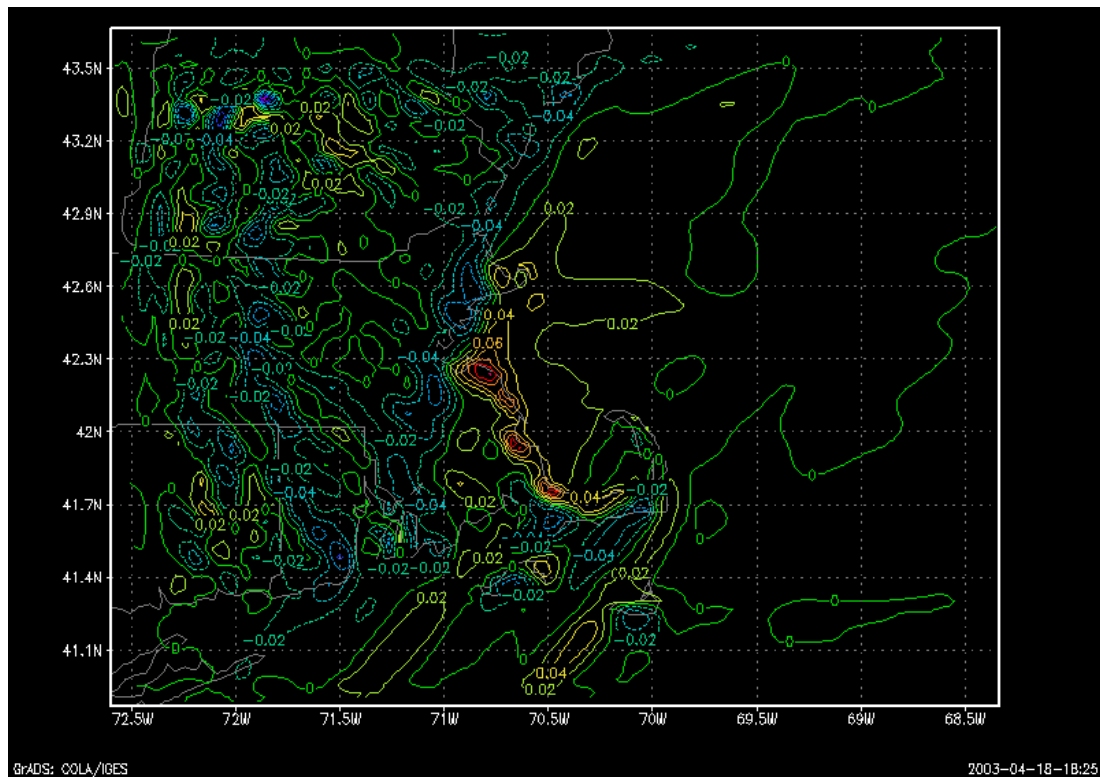


Figure 18. As in Fig. 11, except for 12 UTC, January 14, 1999.

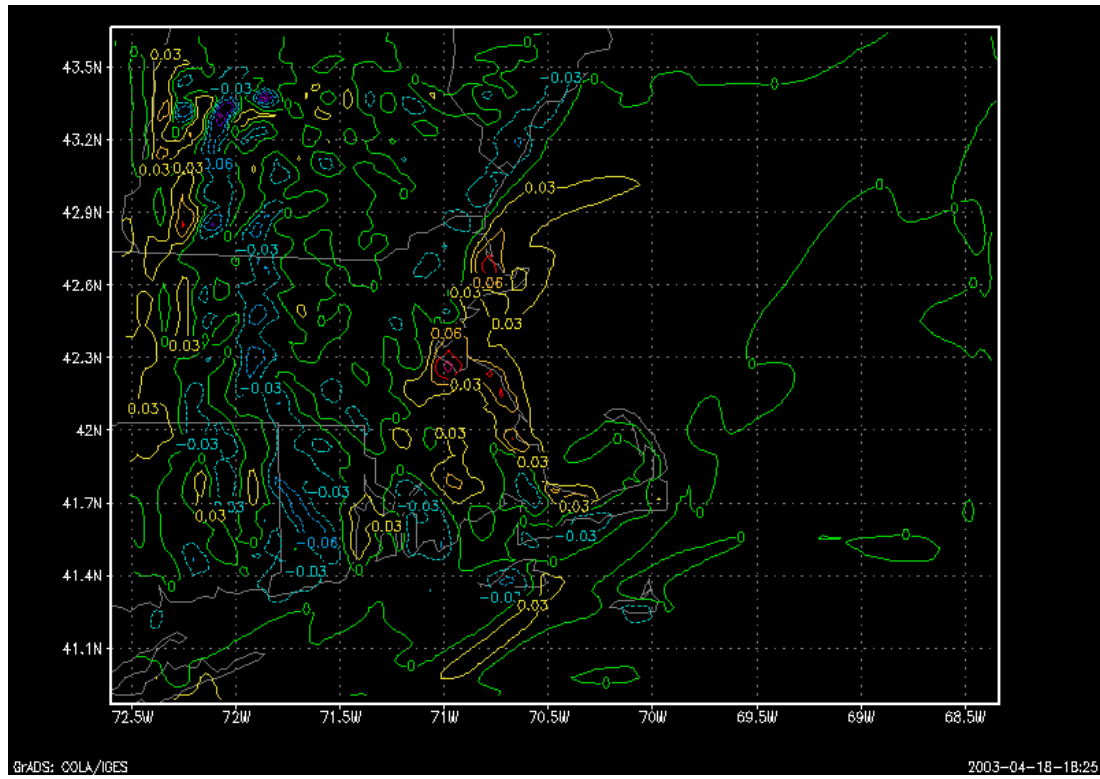


Figure 19. As in Fig. 18, except for 18 UTC.

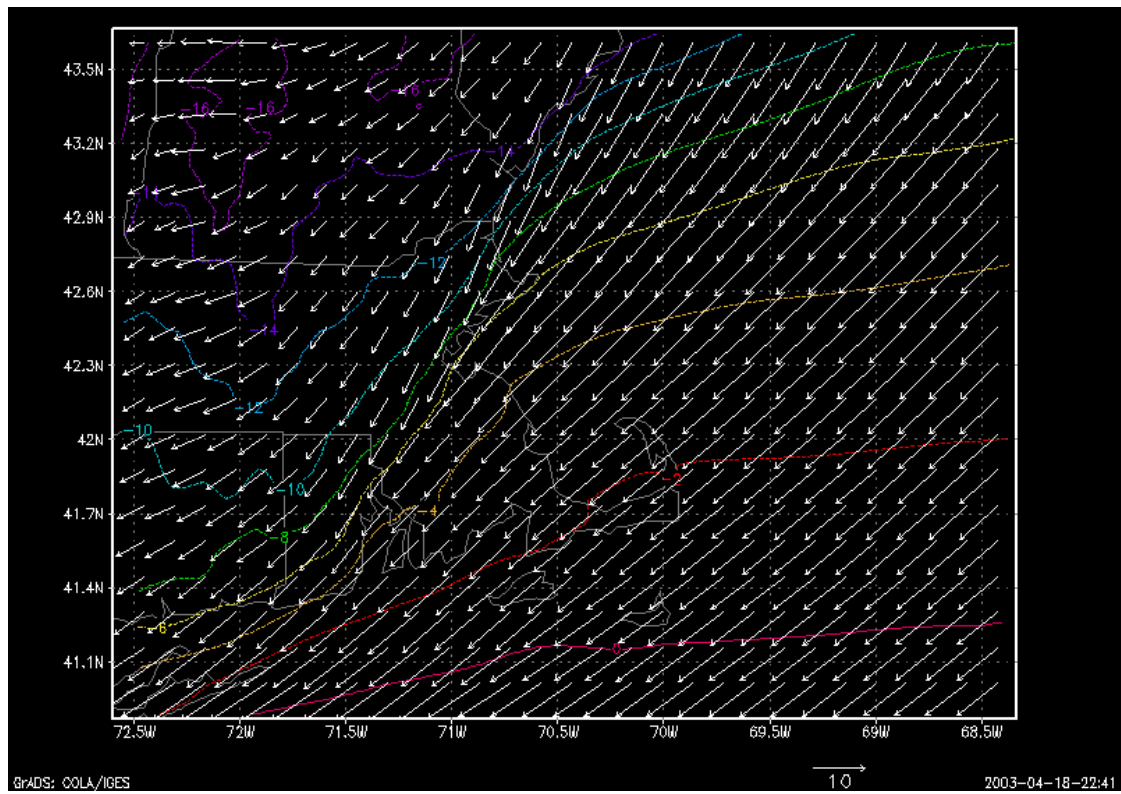


Figure 20. As in Fig. 8, except for 18 UTC, January 14, 1999.

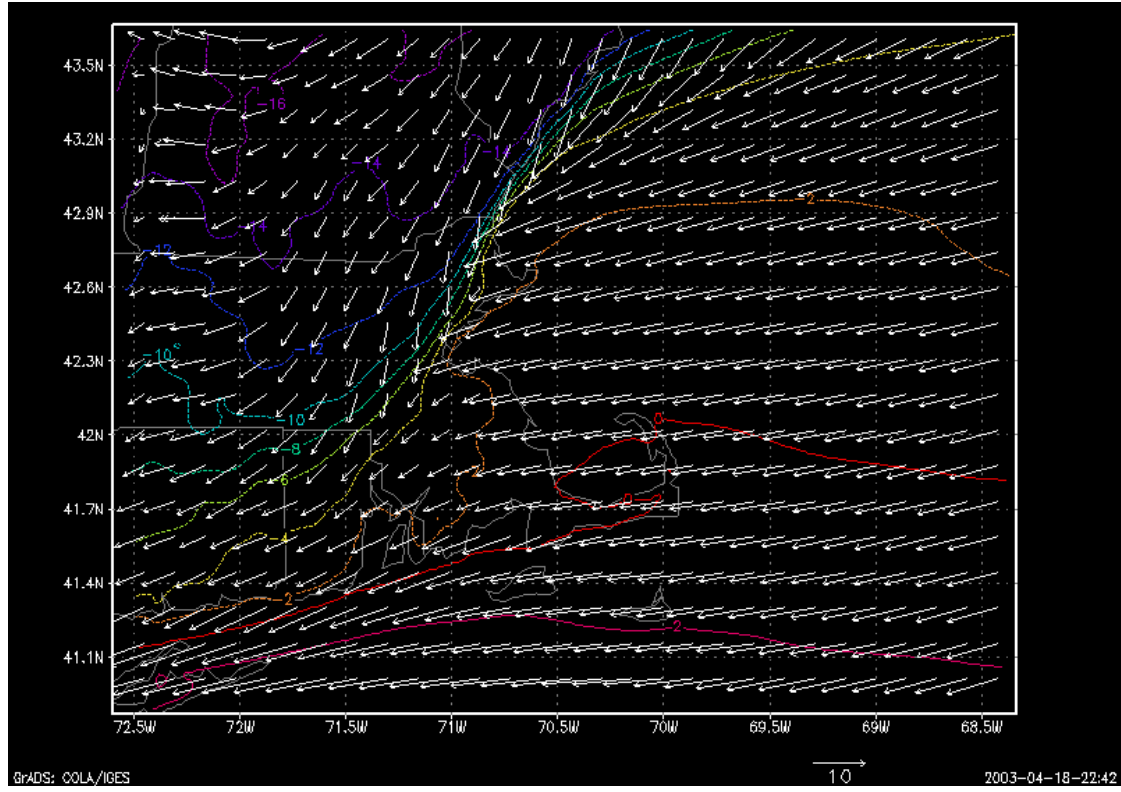


Figure 21. As in Fig. 20, except for 00 UTC, January 15, 1999.

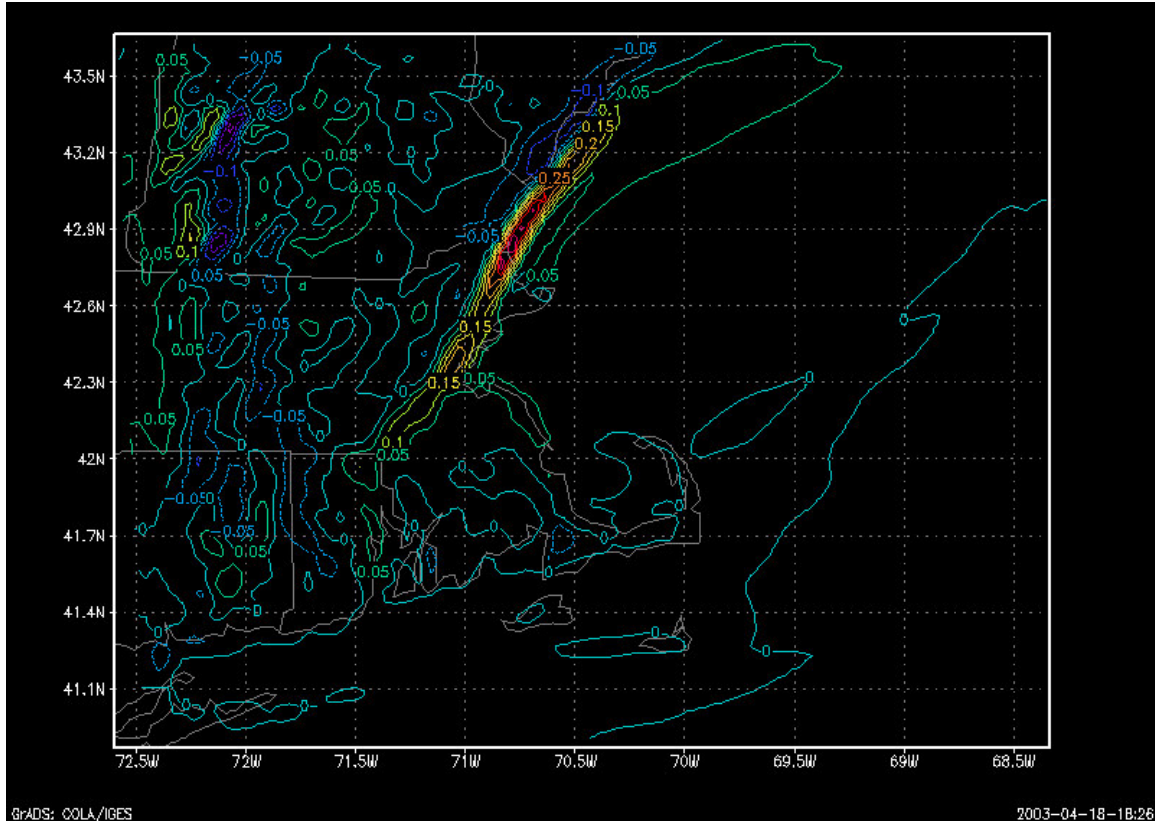


Figure 22. As in Fig. 19, except for 00 UTC, January 15, 1999.

The MM5 simulation used here to document these bands was clearly able to simulate these structures. It is not clear yet whether these simulated bands were correctly timed and placed, since comparison with observations has not been completed. More work will be done to determine the mode of instability in each of these bands as well.

6. Acknowledgements

This work has been helped considerably by scripts written by Mr. Matt Jones while a senior undergraduate, and Ms. Susanna Hopsch while a M.S. student.

7. References

Dudhia, J., 1989: Numerical study of convection observed during the Winter Monsoon Experiment using a mesoscale two-dimensional model. *J. Atmos. Sci.*, **46**, 3077–3107.

Grell, G. A., 1993: Prognostic evaluation of assumptions used by cumulus parameterizations. *Mon. Wea. Rev.*, **121**, 764–787.

Hong, S.-Y., and H.-L. Pan, 1996: Nonlocal boundary layer vertical diffusion in a medium-range forecast model. *Mon. Wea. Rev.*, **124**, 2322–2339.